A NOVEL p.Asp304Gly MUTATION IN *BEST1* GENE ASSOCIATED WITH ATYPICAL BEST VITELLIFORM MACULAR DYSTROPHY PHENOTYPE AND HIGH INTRAFAMILIAL VARIABILITY

ENRICO PEIRETTI, MD,* GIULIA CAMINITI, MD,* GINA FORMA, MD,* GIOVANNELLA CARBONI, MD,* CLAIRE-MARIE DHAENENS, MD,† LEA QUERQUES, MD,‡ ERIC SOUIED, MD, PhD,§¶ GIUSEPPE QUERQUES, MD, PhD‡§

Purpose: To report the atypical phenotypic characteristics of patients with a novel p.Asp304Gly mutation in *BEST1*.

Methods: Affected individuals underwent a complete ophthalmic examination, including best-corrected visual acuity, fundus autofluorescence, spectral domain optical coherence tomography, and electrophysiologic testing. All individuals were screened for mutations in the *BEST1* gene.

Results: Five patients of the same Italian family were clinically examined. All patients complained of decreased vision as the initial symptom. Best-corrected visual acuity ranged from 20/800 to 20/32. On fundus examination, all patients showed atypical Best vitelliform macular dystrophy phenotype with multifocal macular and extramacular involvement. The spectral domain optical coherence tomography characteristics of central macular and extramacular lesions varied in each patient and included "giant" choroidal excavation, extensive flat macular elevation with hyporeflective subretinal material accumulation surrounded by hyperautofluorescent spots/annulus, and extensive hypoautofluorescent extramacular atrophic areas. Electrooculogram was always abnormal with Arden ratio lower than 1.55, whereas electroretinogram was normal in the two younger patients and abnormal (low amplitude) in the three older patients. Genetic analysis revealed a novel missense mutation in *BEST1*, substituting aspartate for glycine at amino acid 304.

Conclusion: We describe the atypical phenotype and high intrafamilial variability associated with a new mutation in the *BEST1* gene in an Italian family affected with Best vitelliform macular dystrophy. Clinicians should consider screening the *BEST1* gene even in the absence of the typical phenotype and in case of high intrafamilial variability.

RETINA 0:1–8, 2016

Best vitelliform macular dystrophy (VMD) is macular degeneration, inherited as autosomal dominant trait, with incomplete penetrance and very different clinical expression. The onset of Best VMD is usually juvenile but the clinical manifestations of the disease are highly variable from early childhood to the sixth decade of life.[1–3] Best VMD is characterized by an accumulation of lipofuscinlike material resulting in an egg yolk–like shape of the macula; it has been described for the first time by Frederick Best in 1905[4] with a complete report of the various stages of the disease. This abnormal material is associated with progressive macular degeneration, which finally causes a considerable loss of central vision in some patients. The diagnosis can be made in many affected individuals on the basis of the typical appearance of the retinal lesions but clinical evaluations such as fundus autofluorescence (FAF) and optical coherence tomography (OCT) are helpful in the staging of the disease. Abnormal electrooculogram (EOG) with a reduced or nondetectable light-peak to dark-trough ratio associated with a normal clinical electroretinogram (ERG) has been classically considered as necessary for the definition of the disease.[5,6]

The gene involved in Best VMD, called *BEST1*, encodes a protein named bestrophin-1, which is localized to the basolateral plasma membrane of the retinal pigment epithelium (RPE), hypothesized to function as a Ca^{2+}-activated Cl^- channel, or a regulator of ion transport.[7–10]

Best VMD is a clinically variable and pleomorphic disease[11]; usually it begins with symptoms of blurred vision, metamorphopsia, and a reduction of central vision. Most cases have a single lesion in the macula; others have multifocal vitelliform lesions, which are generally limited to the posterior pole.

In this study, we identified affected individuals from the same family with a novel missense mutation in *BEST1*, substituting aspartate for glycine at amino acid 304. Clinical characterization, including FAF, OCT, EOG, and ERG of these individuals, demonstrates atypical Best VMD phenotype and highly variable intrafamilial expression.

Methods

Multiple Italian family members with autosomal dominant Best VMD were studied at the Retinal Center, Eye Clinic, University of Cagliari. The study adhered to the principles of the Declaration of Helsinki and was approved by the Local Ethics Committee. Each patient gave written informed consent.

All individuals underwent a complete ophthalmic examination, including best-corrected visual acuity measurement using standard early treatment of diabetic retinopathy study charts, slit-lamp anterior segment and fundus biomicroscopy, fundus photography (TRC-50IX; Topcon, Inc, Tokyo, Japan), FAF (Spectralis HRA + OCT, Heidelberg Engineering Heidelberg, Germany), spectral domain OCT (Spectralis HRA + OCT; Heidelberg Engineering, Heidelberg, Germany; HD-OCT; OCT 4000 Cirrus; Humphrey-Zeiss, San Leandro, CA), and electrophysiologic tests (EOG, ERG) performed with modular programmable BM 6000-3 MAXI (Biomedica Mangoni S.n.c, Pisa, Italy)—software winAverager for ERG and winEOG for EOG—according to the International Society for Clinical Electrophysiology of Vision Guidelines.[12,13] The ERG was performed after pupil dilation, with tropicamide drops and 20 minutes of dark adaptation: 2 ERG jet electrodes were used for the 2 younger patients after corneal anesthesia with lidocaine while 2 eyelid skin electrodes were used for the 3 older patients; 2 reference electrodes cutaneous temporal and 1 ear clip (grounding) in the right ear lobe. The EOG was performed using 2 channels, applying 4 cutaneous electrodes to the inner canthus and the outer canthus of both eyes, 1 ear clip (grounding) in the right ear lobe (Lighting adaptation: 35 Lux—period 3 minutes; Lighting phase 1: 0 Cd/m^2—period 15 minutes; Lighting phase 2: 400 Cd/m^2—period 15 minutes). In our clinic laboratory, an Arden value of 1.50 provides a meaningful measure with which we discriminate between normal and abnormal tests.

All affected were screened for mutations in the *BEST1* gene by sequencing of the 10 coding exons and their exon–intron boundaries (Table 1) using an ABI 3730 sequencer (Applied Biosystems, Foster City, CA), performed at the molecular biology laboratory in Lille, France. Each polymerase chain reaction was performed in a 25 μL reaction mix containing 25 ng genomic DNA, 1 μM of each primer, and 0.25 U of Taq DNA polymerase (Life Technologies, Carlsbad, CA) or 1.25 U of Taq PCRx DNA polymerase (Life Technologies, Carlsbad, CA) in its appropriate buffer. After the first denaturation at 94°C for 3 minutes, amplification was carried out in 30 or 35 cycles at 94°C for 20 seconds, 60°C for 40 seconds, and 72°C for 45 seconds, ending with a final extension step for 7 minutes. Polymerase chain reaction products were purified with exonuclease (Affymetrix, Santa Clara, CA) and TSap (Promega, Madison, WI). Sequencing of all amplified fragments was performed using the BigDye Terminator Cycle Sequencing Ready Reaction kit V3.1 (Applied Biosystems, Foster City, CA). Sequencing results were analyzed using SeqScape Software Version 2.7 (Applied Biosystems, Foster City, CA).

Results

Five patients (4 men and 1 woman; age, 38–79 years) from the same Italian family (2 generations: 3 brothers affected and the 2 sons of the younger brother) were clinically examined (Figure 1). Summary of the clinical findings of all family members is shown in Table 2.

All patients complained of decreased vision as the initial symptom. Best-corrected visual acuity at

From the *Eye Clinic, University of Cagliari, Cagliari, Italy; †CHRU Lille, Biochemistry and Molecular Biology Department, UF Génopathies, Lille, France; Lille University, Faculté de Médecine, Lille, France; ‡Department of Ophthalmology, IRCCS Ospedale San Raffaele, University Vita-Salute San Raffaele, Milan, Italy; §Department of Ophthalmology, Centre Hospitalier Intercommunal de Creteil, University Paris Est Creteil, Creteil, France; and ¶CRB, Centre de Ressources Biologique, Centre Hospitalier Intercommunal de Creteil, University Paris Est Creteil, Creteil, France.

None of the authors have any financial/conflicting interests to disclose.

Reprint requests: Giuseppe Querques, MD, PhD, Department of Ophthalmology, Centre Hospitalier Intercommunal de Creteil, 40 Avenue de Verdun, 94000 Creteil, France; e-mail: giuseppe.querques@hotmail.it

Table 1. Primers and PCR Reactions

Sequences Amplified	Sense Primers (5′-3′)	Antisense Primers (5′-3′)	PCR Conditions
BEST1 exon 2	GGTCCCTATGGGAGAGTTG	GGACCTGGTCAGGAGCTC	1.5 mM $MgCl_2$, 60°
BEST1 exon 3	CTGGGGAAAATGTGGGATAG	CCCTCAGAAAATGGGGTTTTC	Taq PCR_X DNA polymerase, 60°
BEST1 exon 4	CAGCAGAAAGCTGGAGGAG	CCCATCTTCCATTCCTGCC	Taq PCR_X DNA polymerase, 60°
BEST1 exon 5	AGGTTCCTATAGGTCAGCAG	GGCTCTCGGAAGACCCTC	Taq PCR_X DNA polymerase, 60°
BEST1 exon 6	CACACAGCCAGGAATGGAC	CTTCAAAGTGTGGACCCAAC	1.5 mM $MgCl_2$, 60°
BEST1 exon 7	CATCCTGATTTCAGGGTTCC and CTGGAGGCATGGCCAGAG nested	CTCTGGCCATGCCTCCAG	Taq PCR_X DNA polymerase, 60°
BEST1 exon 8	ATGGGGTGTGGAAATAGCAG	GAGGGGAAGGGTTGATCATT	1.5 mM $MgCl_2$, 60°
BEST1 exon 9	CAGGGAAACTGAGGTCCAG	GTGCCTGACACTTACTGAAG	Taq PCR_X DNA polymerase, 60°
BEST1 exon 10a	TGGGCCAACTGAGAGAGAG	TGGTTCTAGGGGGAAGAACA	1.5 mM $MgCl_2$, 60°
BEST1 exon 10b	ACAAGGCAGCCAAACAGAAC	GTGTGCTCTGGCAGTGATG	Taq PCR_X DNA polymerase, 60°
BEST1 exon 11	ACCTTTGCCCTCCTACTGC	AAGGGTTCCCGACTCTGAAT	Taq PCR_X DNA polymerase, 60°

PCR, polymerase chain reaction.

presentation ranged from 20/800 to 20/32, thereby being lower in the first generation of the family (i.e., the older patients). The anterior segments and intraocular pressure were within normal limits. On fundus examination, all patients showed atypical Best VMD phenotype with multifocal macular and extramacular involvement.[3]

Electrooculogram testing was always abnormal with Arden ratio lower than 1.55, whereas ERG testing was normal in the two younger patients (the second generation of the family) and abnormal (low amplitude) in the three older patients (the first generation of the family), as compared with age-matched control subjects.

The central macular lesions varied from typical accumulation of yellowish vitelliform material (Figure 2) to round/oval, hypopigmented atrophic/fibrotic scars (with or without residual yellowish material), along with some hypertrophy of the RPE and pigment accumulation (Figures 2–6). Extramacular lesions varied in number, size, and appearance from large, well-circumscribed yellowish (similar to the central lesion) (Figure 2) to small diffuse lesions with irregular yellowish deposits (Figures 2–6). The extramacular lesions were mostly located superiorly to the optic disk and along the superotemporal vascular arcades (Figures 2–6).

Fundus autofluorescence revealed increased autofluorescence in correspondence of the yellowish material as seen on fundus biomicroscopy. The central macular lesion appeared as a hyperautofluorescent round lesion (Figure 2), whereas the extramacular lesions appeared either as a large (isolated and

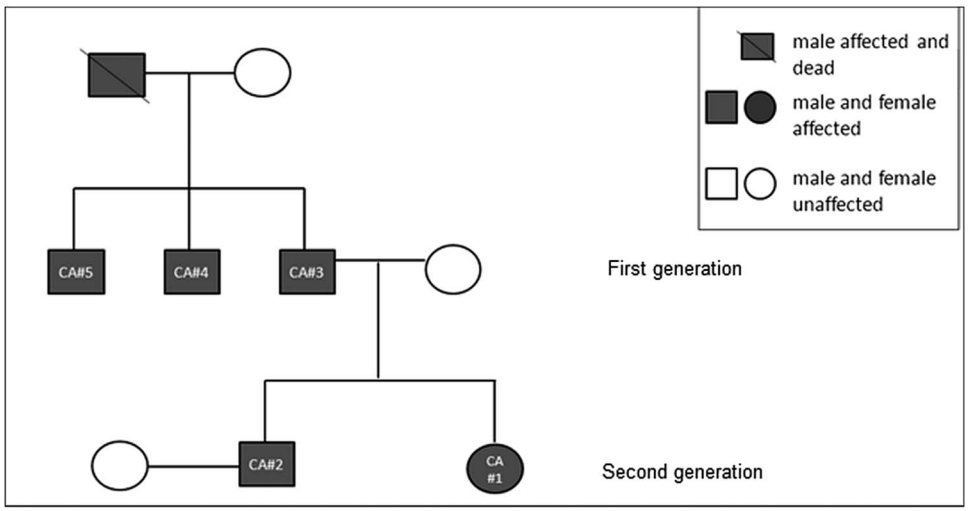

Fig. 1. Pedigree of the family studied. Three brothers are affected by Best VMD; both sons of the younger brother are also affected.

Table 2. Summary of the Clinical Findings for the 5 Patients Affected With Atypical Best VMD

Patient	Age (years)	Gender	BCVA OD	EOG Arden Ratio OD	BCVA OS	EOG Arden Ratio OS	ERG	Mutation	Effect
CA#1	38	F	20/50	1.35	20/32	1.40	Normal	c.911A>G	p.Asp304Gly
CA#2	40	M	20/32	1.41	20/50	1.43	Normal	c.911A>G	p.Asp304Gly
CA#3	71	M	20/200	1.07	20/60	1.18	Abnormal*	c.911A>G	p.Asp304Gly
CA#4	73	M	20/200	1.10	20/200	1.20	Abnormal*	c.911A>G	p.Asp304Gly
CA#5	79	M	20/800	1.02	20/200	1.24	Abnormal*	c.911A>G	p.Asp304Gly

Arden Ratio for the laboratory. Normal EOG: >1.50; Probably normal EOG: 1.41 to 1.51; Probably subnormal EOG: 1.36 to 1.40; Subnormal EOG: 1.06 to 1.35; Flat EOG: 1.00 to 1.05.

*The examination revealed normal morphology and latency time in both eyes, but low amplitude, as compared with age-matched control subjects.

BCVA, best-corrected visual acuity; F, female; M, male; OD, right eye; OS, left eye.

well-circumscribed) highly hyperautofluorescent lesion (Figure 2) or as hyperautofluorescent spots (Figures 3–6). Atrophic/fibrotic scars (Figure 3), areas of hypertrophy of the RPE and pigment accumulation appeared as hypoautofluorescent (Figures 3–4).

Spectral domain optical coherence tomography revealed either hyperreflective or hyporeflective subretinal material accumulation responsible for variable elevation of the central retina (from dome-shaped to extensive, flat macular elevation) (Figures 2–6). Atrophic scars were characterized by loss of outer retinal layers (including the outer nuclear layer, external limiting membrane, ellipsoid zone, and interdigitation), whereas fibrotic scars, areas of hypertrophy of the RPE and pigment accumulation appeared as outer, retinal hyperreflective lesions with variable loss of outer retinal layers (Figures 3–4).

It is interesting to note that despite age being fairly constant in the two generations of the family, there was high phenotypic variability not only between but also within generations.

Patient CA#1, from the second generation of the family, better represented the phenotypic trait of typical Best VMD, except for the multifocal appearance of the right eye lesion because of the presence of an extramacular (temporal to the macula) hyperautofluorescent area (Figure 2).

Patient CA#2, belonging to the second generation of the family, had a multifocal appearance because of the presence of an extramacular hyperautofluorescent deposit and showed a very peculiar phenotype because the macula of both eyes revealed a characteristic choroidal excavation, and in 1 eye appeared as "giant," involving the entire macular area (Figure 3).[14]

Patient CA#3, from the first generation of the family, had multifocal bilateral atrophic/fibrotic scars, responsible for central macular and extramacular

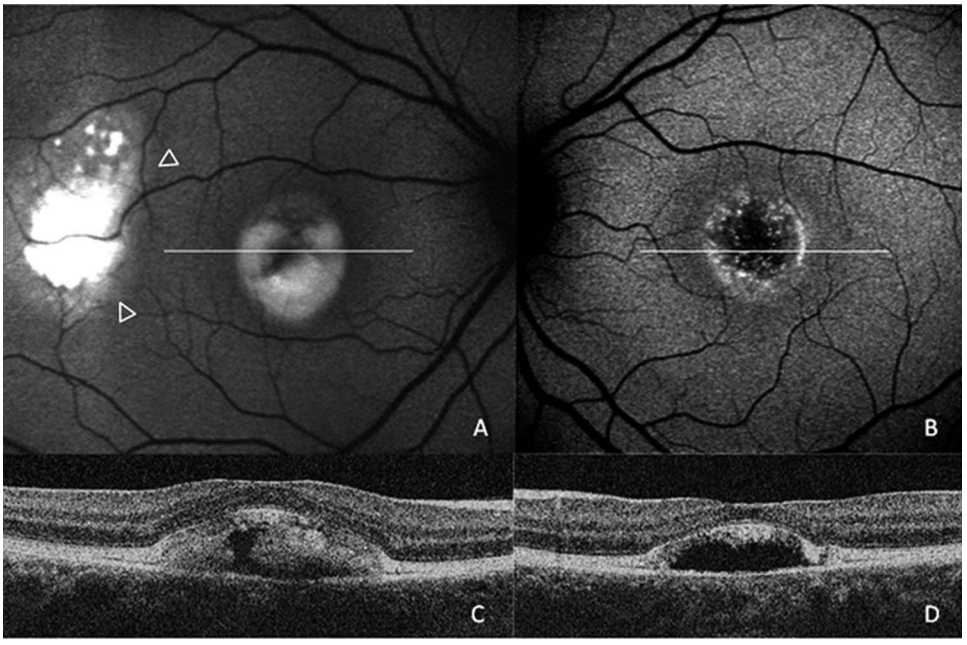

Fig. 2. Fundus autofluorescence and spectral domain OCT of patient CA #1. Fundus autofluorescence shows in the right eye a central macular hyperautofluorescent round lesion (corresponding to the typical round accumulation of yellowish vitelliform material), along with a large (isolated and well-circumscribed) highly hyperautofluorescent lesion (arrowhead) located temporally to the central macular lesion (**A**). In the left eye, FAF reveals a central, macular hypoautofluorescent round lesion surrounded by hyperautofluorescent spots (**B**). Spectral domain OCT scans reveal hyperreflective subretinal material accumulation in the right eye (**C**), and hyporeflective subretinal material accumulation in the left eye (**D**), responsible for a dome-shaped elevation of the central retina.

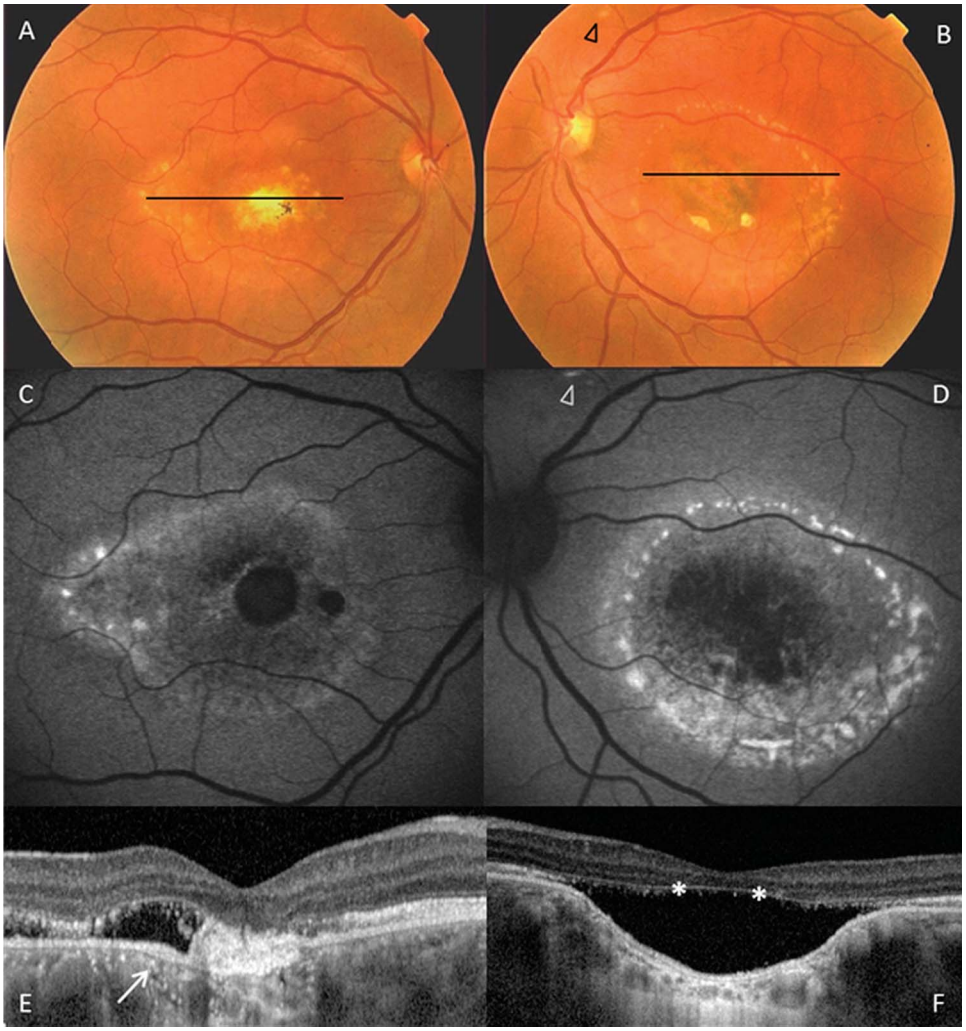

Fig. 3. Color fundus photograph, FAF, and spectral domain OCT of patient CA #2. Color fundus photographs show round/oval, hypopigmented atrophic/fibrotic scars (**A** and **B**). In the left eye, small lesions with irregular yellowish (hyperautofluorescent) deposits are located along the superotemporal vascular arcades (**B** and **D**; arrowhead). Fundus autofluorescence reveals a central, macular hypoautofluorescent round lesion surrounded by hyperautofluorescent spots (**C** and **D**). Spectral domain OCT shows a "focal" choroidal excavation in the right eye (arrow), associated with hyperreflective fibrotic scar (characterized by loss of outer retinal layers) with some hyporeflective subretinal material, and a "giant" choroidal excavation in the left eye, occupying the whole macular area and associated with hyporeflective subretinal material (**E** and **F**). Note the loss of ellipsoid zone and interdigitation zone in areas of choroidal excavation (**E** and **F**; asterisks).

hypoautofluorescent lesions surrounded by hyperautofluorescent spots (Figure 4).

Patients CA#4 and CA#5, belonging to the first generation of the family, showed extensive flat macular elevation because of hyporeflective subretinal material accumulation, and an inhomogeneous hyperautofluorescent surrounding the central hypoautofluorescent, which in both eyes of patient CA#4 took the shape of an annulus (Figure 5). Interestingly, the right eye of patient CA#5 showed an extensive and irregular hypoautofluorescent atrophic area all around the optic disk (Figure 6).

Analysis revealed a novel missense mutation in *BEST1*, substituting aspartate for glycine at amino acid 304, not identified in 96 control individuals.[11] This mutation is not reported in the literature but the amino acid 304 is already described in the substitutions p.Asp304Ile and p.Asp304Val.[15,16] Asp304 is located in the acidic domain, in the C terminus of the protein, and belongs to a cluster of 5 amino acids (293–308) crucial for normal channel gating by $Ca^{(2+)}$.[17] The physical-chemical distance between the aspartic acid residue and the glycine residue is important. The mutation affects very conserved nucleotide and amino acid, and *in silico* prediction software (Polyphen [Harvard University, Boston, MA], SIFT [J. Craig Venter Institute, Rockville], and GVGD [IARC, Lyon, France]) predicts this mutation as probably damaging.

Discussion

Best VMD is an inherited macular dystrophy, and its phenotype can be extremely variable even among members of a single family. In this report, we describe the atypical Best VMD presentation in 5 affected individuals belonging to the same Italian family (Figure 1), all showing the same novel missense mutation in *BEST1* (causing a change at the position 304 of aspartate to glycine). Despite the fact that each

Fig. 4. Color fundus photograph, FAF, and spectral domain OCT of patient CA #3. Color fundus photographs show round/oval, hypopigmented atrophic/fibrotic scars (**A** and **B**), along with some hypertrophy of the RPE and pigment accumulation (arrowheads). Fundus autofluorescence reveals an area of inhomogeneous geographic hyperautofluorescent (arrows) surrounding the atrophic hypoautofluorescent scars (**C** and **D**). On spectral domain OCT, areas of hypertrophy of the RPE and pigment accumulation appeared as outer retinal hyperreflective lesions with variable loss of outer retinal layers (**E** and **F**).

member of the family presented the same autosomal mutation and the genetic analysis did not show any other mutation in the *BEST1* gene, the phenotypic presentations were definitely variables (accounting for a highly variable intrafamilial expression).

The best-corrected visual acuity at presentation ranged from 20/800 to 20/32, thereby being lower in the older subjects (the first generation of the family). Similarly, ERG testing was abnormal (low amplitude) only in the 3 older patients (the first generation of the family), whereas EOG testing was typically abnormal with Arden ratio lower than 1.55 in all subjects.

The age was fairly constant in the two generations of the family; however, the phenotype was highly variable not only between but also within generations.

All patients showed atypical Best VMD phenotype with multifocal macular and extramacular involvement (mostly located superiorly to the optic disk and along the superotemporal vascular arcades).[3] In 1 eye of a patient from the second generation of the family, the extramacular yellowish lesion was large, isolated, and well-circumscribed, located temporally to the central macular lesion (Figure 2).

In 3 eyes of 2 patients, both from the second generation of the family, FAF revealed a central, macular hypoautofluorescent round lesion surrounded by hyperautofluorescent spots (Figures 2–3). This highlights how extramacular lesions have the same characteristics as the central macular lesions,[18] although, as reported by Boon et al,[3] the stages between the lesions could differ. Interestingly, in 6 eyes of 3 patients, all belonging to the first generation of the family, FAF showed an area of inhomogeneous geographic hyperautofluorescent surrounding the central hypoautofluorescent (Figures 4 and 6), which in 2 eyes of a patient took the shape of an annulus (similar to the annulus typically found on FAF in cone–rod and other retinal dystrophies)[19] (Figure 5). One eye of a patient from the first generation of the family showed

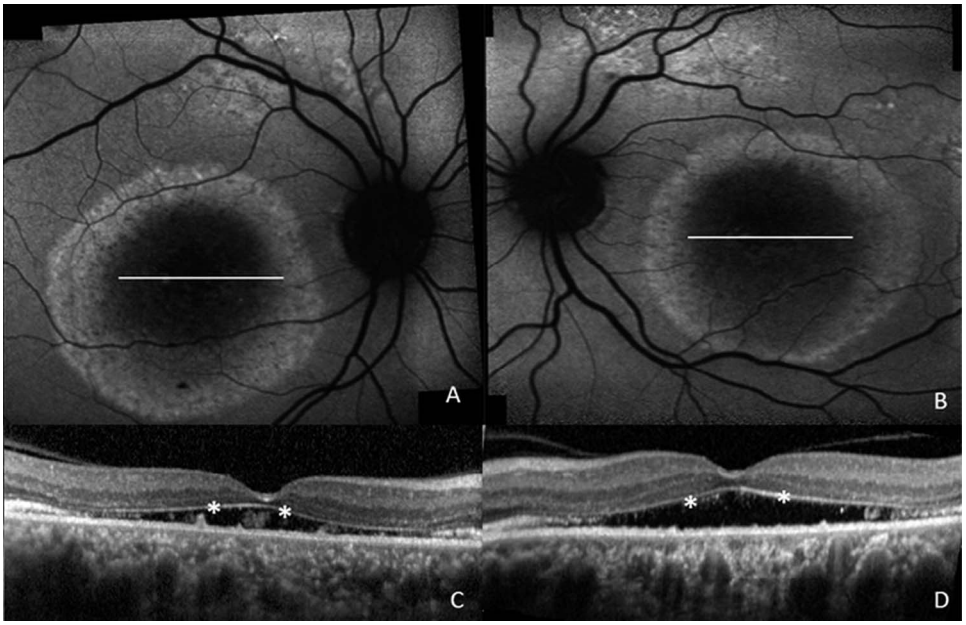

Fig. 5. Fundus autofluorescence and spectral domain OCT of patient CA #4. Fundus autofluorescence reveals an annulus of inhomogeneous hyperautofluorescent surrounding the central hypoautofluorescent (**A** and **B**). Spectral domain OCT shows elevation of the central retina due to extensive, flat hyporeflective subretinal material accumulation (**C** and **D**). Note the loss of ellipsoid zone and interdigitation zone in areas of extensive, flat macular elevation (**C** and **D**; asterisks).

an extensive and irregular hypoautofluorescent atrophic area all around the optic disk (Figure 6).

In both eyes of the same patient from the second generation of the family, spectral domain OCT revealed a choroidal excavation, which was "focal" in 1 eye (and associated with hyperreflective fibrotic scar with some hyporeflective subretinal material) and "giant" (occupying the whole macular area and associated with hyporeflective subretinal material) in 1 eye (Figure 3). A similar much less prominent excavation has been recently reported by Parodi et al[14] in both eyes of a patient issuing from a family affected with Best VMD because of a mutation in the *BEST1* gene (c.73C > T [p.Arg25Trp]). It is noteworthy that loss of ellipsoid zone and interdigitation (but not outer nuclear layer and external limiting membrane) was detected in areas of choroidal excavation (Figure 3) and of extensive flat macular elevation (Figures 5–6).

According to Boon et al,[3] the phenotypic characteristics of patients affected by Best VMD could be various and sometimes can simulate different other macular dystrophies. The wide variability in the

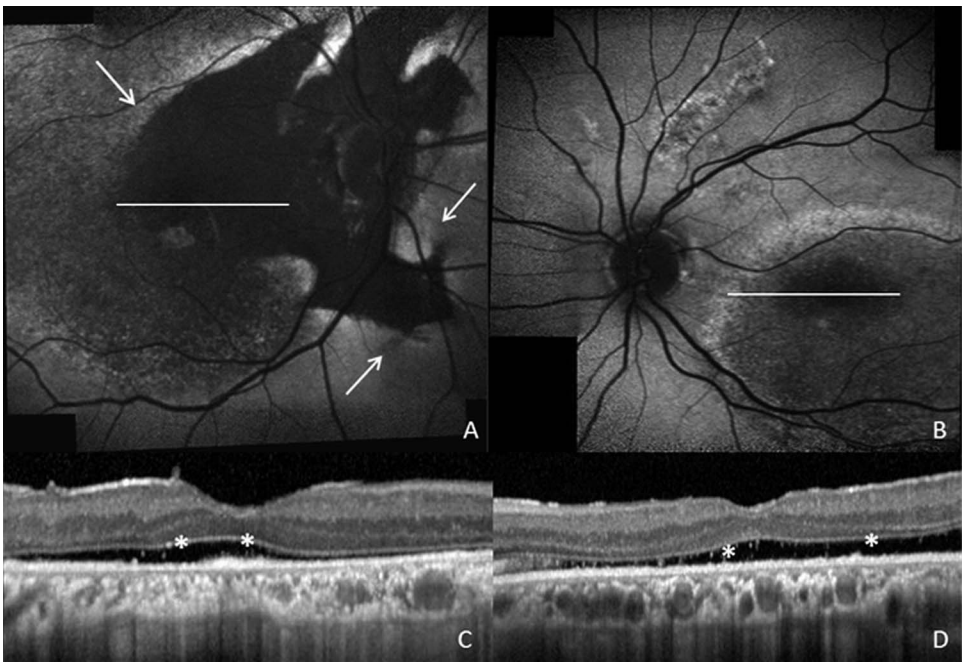

Fig. 6. Fundus autofluorescence and spectral domain OCT of patient CA #5. Fundus autofluorescence reveals an area of inhomogeneous geographic hyperautofluorescent (arrows) surrounding the atrophic hypoautofluorescent scars (**A** and **B**), extending, in the left eye, all around the optic disk (**B**). Spectral domain OCT shows elevation of the central retina due to extensive, flat hyporeflective subretinal material accumulation (**C** and **D**). Note the loss of ellipsoid zone and interdigitation zone in areas of extensive flat macular elevation (**C** and **D**; asterisks).

phenotypic appearance of our series may be due to environmental factors or modifying genes.[20] As we did not perform an extensive genetic analysis, we cannot rule out other genetic components in our family.

Best VMD typically causes lesions at the posterior pole; however, histopathology has shown extensive abnormalities of the RPE, Bruch membrane, and the choroid throughout the fundus.[21–24] We hypothesize that the novel mutation in the *BEST1* gene found in our series can be responsible for a more severely affected RPE and thus lead to the formation of extramacular lesions and other peculiar findings, including "giant" choroidal excavation, extensive flat macular elevation with hyporeflective subretinal material accumulation surrounded by hyperautofluorescent spots/annulus, and extensive hypoautofluorescent extramacular atrophic areas.

In conclusion, we report on a new *BEST1* mutation associated with atypical phenotype and high intrafamilial variability. To make appropriate prognostic considerations, clinicians should consider screening the *BEST1* gene for mutation even in the absence of typical Best VMD phenotype and in case of high intrafamilial variability. Moreover, although currently there is no therapy that stops the evolution of the disease or restores the vision, human gene therapy trials will hopefully shortly be launched for *BEST1*-related disease.

Key words: Best disease, *BEST1* gene mutation, electrophysiology, fundus autofluorescence, genotype, macular dystrophy, optical coherence tomography, phenotype, retinal dystrophy, vitelliform macular dystrophy.

References

1. Godel V, Chaine G, Regenbogen L, et al. Best's vitelliform macular dystrophy. Acta Ophthalmol Suppl 1986;175:1–31.
2. Deutman AF, Hoyng CB. Macular dystrophies. In: Ryan SJ, eds. Retina. 3rd ed. St. Louis, MO: Mosby; 2001:1210–1257.
3. Boon CJ, Klevering BJ, den Hollander AI, et al. Clinical and genetic heterogeneity in multifocal vitelliform dystrophy. Arch Ophthalmol 2007;125:1100–1106.
4. Best F. Ueber eine hereditare Maculaaffektion: beiträge zur Vererbungslehre. Z Augenheilkd 1905;13:199–212.
5. Deutman AF. Electro-oculography in families with vitelliform dystrophy of the fovea. Detection of the carrier state. Arch Ophthalmol 1969;81:305–316.
6. Cross HE, Bard L. Electro-oculography in Best's macular dystrophy. Am J Ophthalmol 1974;77:46–50.
7. Stone EM, Nichols BE, Streb LM, et al. Genetic linkage of vitelliform macular degeneration Best's disease to chromosome 11q13. Nat Genet 1992;1:246–250.
8. Petrukhin K, Koisti MJ, Bakall B, et al. Identification of the gene responsible for Best macular dystrophy. Nat Genet 1998;19:241–247.
9. Sun H, Tsunenari T, Yau KW, et al. The vitelliform macular dystrophy protein defines a new family of chloride channels. Proc Natl Acad Sci U S A 2002;99:4008–4013.
10. Marmorstein AD, Cross HE, Peachey NS. Functional roles of bestrophins in ocular epithelia. Prog Retin Eye Res 2009;28:206–226.
11. Querques G, Zerbib J, Santacroce R, et al. Functional and clinical data of Best vitelliform macular dystrophy patients with mutations in the BEST1 gene. Mol Vis 2009;15:2960–2972.
12. Marmor MF, Fulton AB, Holder GE, et al; International Society for Clinical Electrophysiology of Vision. ISCEV Standard for full-field clinical electroretinography (2008 update). Doc Ophthalmol 2009;118:69–77.
13. Marmor MF, Brigell MG, McCulloch DL, et al; for the International Society for Clinical Electrophysiology of Vision. ISCEV standard for clinical electro-oculography (2010 update). Doc Ophthalmol 2011;122:1–7.
14. Parodi MB, Zucchiatti I, Fasce F, et al. Bilateral choroidal excavation in best vitelliform macular dystrophy. Ophthalmic Surg Lasers Imaging Retina 2014;45:e8–e10.
15. Kinnick TR, Mullins RF, Dev S, et al. Autosomal recessive vitelliform macular dystrophy in a large cohort of vitelliform macular dystrophy patients. Retina 2011;31:581–595.
16. Maia-Lopes S, Silva ED, Reis A, et al. Retinal function in best macular dystrophy: relationship between electrophysiological, psychophysical, and structural measures of damage. Invest Ophthalmol Vis Sci 2008;49:5553–5560.
17. Xiao Q, Prussia A, Yu K, et al. Regulation of bestrophin Cl channels by calcium: role of the C terminus. J Gen Physiol 2008;132:681–692.
18. Querques G, Regenbogen M, Soubrane G, et al. High-resolution spectral domain optical coherence tomography findings in multifocal vitelliform macular dystrophy. Surv Ophthalmol 2009;54:311–316.
19. Robson AG, Michaelides M, Saihan Z, et al. Functional characteristics of patients with retinal dystrophy that manifest abnormal parafoveal annuli of high density fundus autofluorescence: a review and update. Doc Ophthalmol 2008;116:79–89.
20. Boon CJ, Klevering BJ, Leroy BP, et al. The spectrum of ocular phenotypes caused by mutations in the BEST1 gene. Prog Retin Eye Res 2009;28:187–205.
21. Mullins RF, Oh KT, Heffron E, et al. Late development of vitelliform lesions and flecks in a patient with Best disease: clinicopathologic correlation. Arch Ophthalmol 2005;123:1588–1594.
22. Frangieh GT, Green WR, Fine SL. A histopathologic study of Best's macular dystrophy. Arch Ophthalmol 1982;10:1115–1121.
23. O'Gorman S, Flaherty WA, Fishman GA, et al. Histopathologic findings in Best's vitelliform macular dystrophy. Arch Ophthalmol 1988;106:1261–1268.
24. Weingeist TA, Kobrin JL, Watzke RC. Histopathology of Best's macular dystrophy. Arch Ophthalmol 1982;100:1108–1114.